Design Guide: TIDA-060040

Absolute Angle Encoder Reference Design With Hall-Effect Sensors for Precise Motor Position Control

Description

This reference design demonstrates a method for absolute angle encoding typical in precision motor control applications such as robotic arm control. Angle encoding can be achieved using various magnetic sensing technologies. This is done by detecting two magnetic flux density, B-field, vector components which are naturally 90° out of phase. As the magnet spins, the sensor inputs are sinusoidal which allows for calculations using trigonometric properties. However, due to electrical and mechanical characteristics of the system, it is often necessary to correct the final result to achieve the greatest accuracy. Typically in most precision motor control applications, the final target error is less than 0.1°. This design explores the process for selecting a magnet, determining placement, and correcting for system-level imperfections to achieve a highly-accurate angle measurement.

Features

- Measure angle in on-axis, in-plane, and off-axis alignments for flexible alignment and sensor placement
- Calibration process for accuracy of 0.1°
- Selectable digital SPI communication or analog output
- Design files with sensor placement guidance

Applications

- Mobile robot motor control
- Mobile robot sensing module
- Robotic lawn mower
- Robot servo drive
- Servo drive position sensor
- Position sensors
- Self-balancing personal transporter

Resources

TIDA-060040	Design Folder
TMAG5170	Product Folder
DRV5055	Product Folder

Ask our TI E2E™ support experts

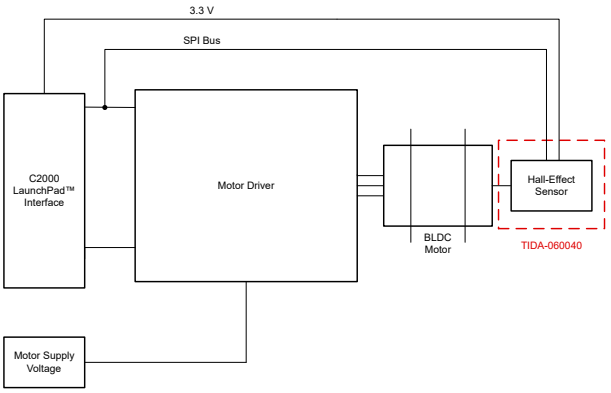

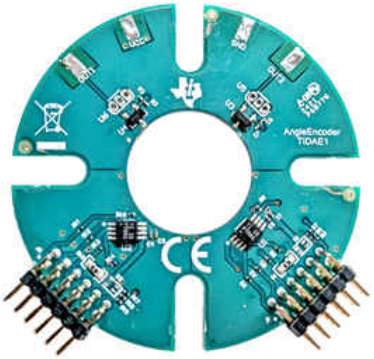

Copyright © 2022 Texas Instruments Incorporated

1 System Description

In any precision motor control application it becomes necessary to assess angular position of the motor shaft to ensure overall control of the system matches expectation. Inaccurate position data may result with impaired user safety, wider manufacturing tolerances and yield loss, navigation failures, or damaged equipment. As a result, it becomes essential in many applications to constantly monitor and evaluate angular position. For example, in autonomous mobile robots and robotic lawnmowers, the ability to match the angular rotation speed of each wheel is critical for proper navigation.

Although various technologies exist for angle measurement, this design demonstrates the use of two standard one dimensional (1D) linear Hall-effect sensors or a three dimensional (3D) linear Hall-effect sensor. Each technique is subject to various challenges which must be addressed.

Table 1-1. Angle Measurement Methods

METHOD	ADVANTAGES	DISADVANTAGES
3D Hall-effect (Method demonstrated in this design)	• Single sensor can capture entire magnetic field • Sensor placement is flexible for compact solutions • Angle position is available at system power up • Immune to dirty working conditions	• Depending on range and placement, magnetic field may be non-ideal • Magnet cost
1D Hall-effect (Method demonstrated in this design)	• Inexpensive sensors with analog output • Compact solution size • Angle position available at system power up • Immune to dirty working conditions	• Requires precise sensor placement for accurate phase alignment • Magnet cost
Hall-effect Incremental Encoding	• Captures speed and direction of rotating magnet • Simple calculation for incremental angle changes • Immune to dirty working conditions	• Requires a multipole ring magnet • Provides incremental angle position only and position at power up is unknown
Inductive Sensed Angle Encoding	• Immune to influence from nearby fixed permanent magnets • Immune to dirty working conditions	• Requires precise design of sense coil and metal target
Optical Encoding	• Provides highest resolution data	• Solution size tends to be bulky • Must operate in clean conditions
Stepper Motor Pulse counting	• Simple implementation • Precision control can be achieved using geared configurations	• Step size jitter provides uncertainty in absolute position • Start position is unknown
Sensorless Motor Control	• Does not require additional sensing components	• Does not detect Motor position when stopped • Does not work well at low speeds • Can be difficult to manage at very high speeds • Requires complex calculations

Not all solutions are able to use optical encoding due to contaminants such as dust, dirt, and grime. Optical solutions tend to become bulky to create sealed environments for the sensor, which do not fit well into compact designs.

For inductive and linear Hall-effect based solutions, the premise of the angle calculation uses sinusoidal outputs which are 90° out of phase from each other.

Copyright © 2022 Texas Instruments Incorporated

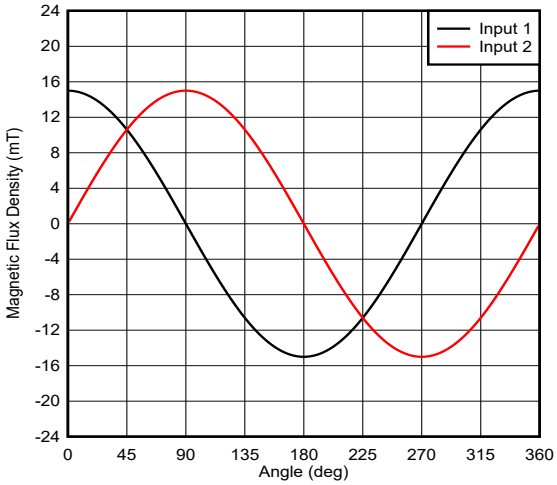

Figure 1-1. Sine and Cosine Inputs

With outputs of this form, use Equation 1 through Equation 4 to describe the absolute angle.

$$Out1 = \sin\theta \quad (1)$$

$$Out2 = \cos\theta \quad (2)$$

$$\tan\theta = \frac{Out1}{Out2} \quad (3)$$

$$\theta = \text{atan}\left(\frac{Out1}{Out2}\right) \quad (4)$$

As Equation 4 shows, determine the angle by calculating the arctangent of the ratio of the two outputs. To simplify this calculation step in software, use the atan2() function available in many coding libraries. This function automatically considers the sign of each input and applies adjustments to produce an output ranging from ±180°.

An additional option is to use a device with an integrated CORDIC calculator. CORDIC is an algorithm that approximates a binary search by performing vector rotations and has been optimized for digital logic. Devices such as TMAG5170 and TMAG5273 are capable of generating angle outputs using the device outputs with minimal total system latency.

Linear Hall-effect solutions may be implemented in the following arrangements, which will be explored in more detail in Sensor Location.

- 1D In-Plane
- 1D Off-Axis
- 3D In-Plane
- 3D Off-Axis
- 3D On-Axis

Copyright © 2022 Texas Instruments Incorporated

2 System Overview

System Specifications

PARAMETER	SPECIFICATION
Operating Voltage	3.0 V–5.5 V (DRV5055A4)
	2.3 V–5.5 V (TMAG5170)
Magnetic Field Input	±85 mT (DRV5055A4)
	±100 mT (TMAG5170)
Output format	0.2 V to Vcc – 0.2 V (DRV5055A4)
	SPI up to 10 MHz
Best Angle Accuracy	< 0.1°

2.1 Block Diagram

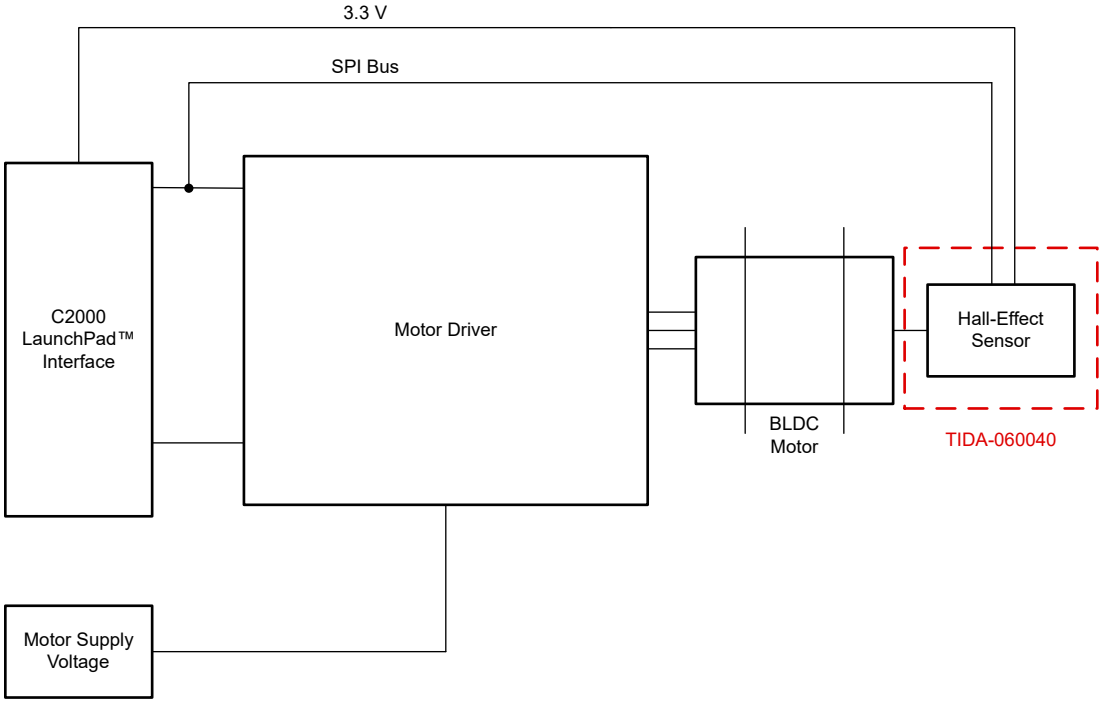

Figure 2-1. TIDA-060040 Block Diagram

2.2 Highlighted Products

2.2.1 TMAG5170

The TMAG5170 is a high-precision linear 3D Hall-effect sensor designed for a wide range of industrial applications. The high level of integration offers flexibility and accuracy in a variety of position sensing systems. This device features 3 independent Hall sensors at X, Y, and Z axes. A precision signal-chain along with an integrated 12- bit ADC enables high accuracy and low drift magnetic field measurements while supporting a sampling of up to 20 kSPS. On-chip temperature sensor data is available for system-level drift compensation.

2.2.2 DRV5055A4

The DRV5055 is a linear Hall-effect sensor that responds proportionally to magnetic flux density. The device can be used for accurate position sensing in a wide range of applications. The device operates from 3.3-V or 5-V power supplies. When no magnetic field is present, the analog output drives half of VCC. The output changes linearly with the applied magnetic flux density, and five sensitivity options enable maximal output voltage swing based on the required sensing range. North and south magnetic poles produce unique voltages.

Copyright © 2022 Texas Instruments Incorporated

2.3 Design Considerations

2.3.1 Magnet Selection

The magnet selected for testing was R834DIA, an N42 Grade diametric ring magnet. The magnet is specified with an inner diameter of 4.75 mm (0.1875 in) and an outer diameter of 12.7 mm (0.5 in). The magnet thickness is 6.35 mm (0.25 in).

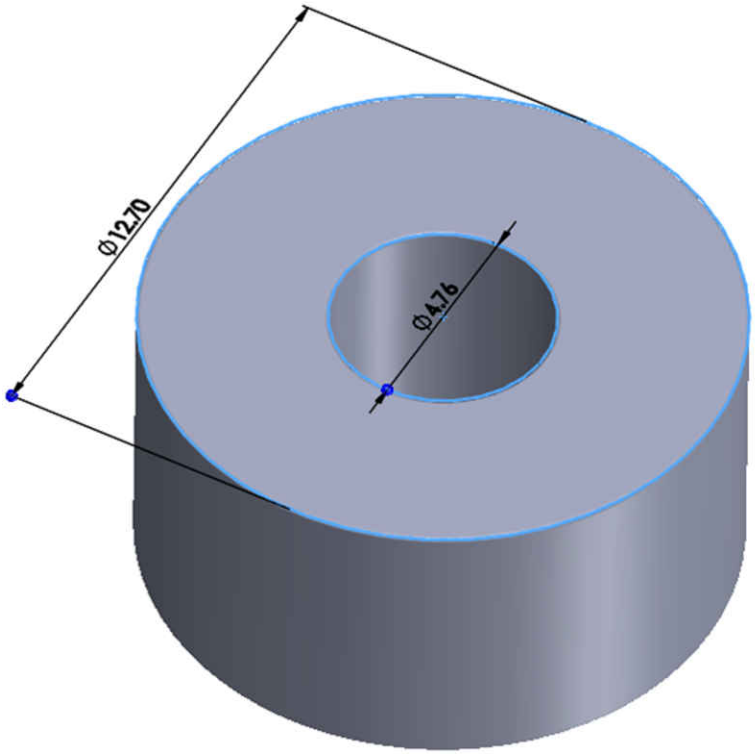

Figure 2-2. Diametric Ring Magnet

2.3.2 Magnet Shape

A ring magnet format was selected for its ability for easily mount to a rotary shaft. Solid cylindrical magnets without a bore hole in the center, must be mounted using a secondary fixture to ensure proper alignment and centering

2.3.3 Magnet Rotation Speed

As the speed of the motorized system increases, this impacts a fixed-phase delay error from the sensor due to the actual propagation delay in the system. The ability of the controller to manage this delay impacts device settings and end performance.

For instance, TMAG5170 offers averaging modes which can help improve the observed input referred noise. Minimizing this noise helps achieve the highest accuracy result, but proportionally increases the overall integration time. This increase in integration time determines the resulting phase-related error.

AVERAGING MODE	SAMPLING PATTERN	TOTAL CONVERSION TIME
1 ×	XY	75 µs
32 ×	XY	1.625 ms
1 ×	XYZZYX	175 µs
32 ×	XYZZYX	4.825 ms

This integration delay can cause speed limitations for a sensor. In the case of the 32 × sampling using the XYZZYX conversion pattern, the total integration time is 4.825 ms. At a motor speed of about 35 RPM, the

Copyright © 2022 Texas Instruments Incorporated

magnet will rotate 1° over the duration of a single conversion. By contrast, comparing the fastest integration time of 75 µs, the magnet would have to spin 64 × faster to similarly rotate by 1° during one conversion.

For any motor, especially when loaded, there must be a deceleration period as the shaft approaches the target position. It is necessary, therefore, to understand the phase delay to predict when to begin the deceleration. As the shaft speed is increased or decreased, the system must account for this delay to accurately understand the actual motor position.

While increased averaging reduces the impact of noise on the measurement, Figure 2-3 demonstrates that the increased sample time results in a greater discrepancy between actual motor shaft angle and the collected data from the sensor.

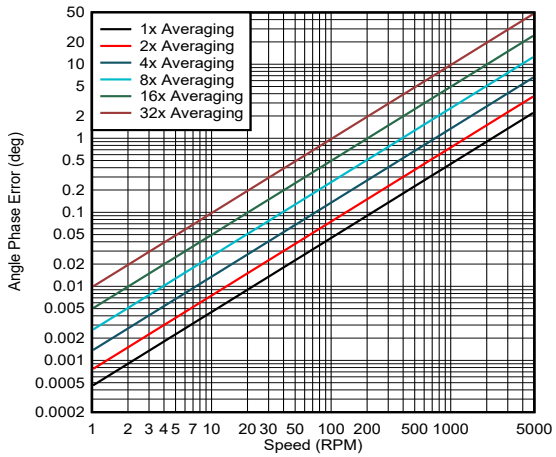

Figure 2-3. Angle Phase Error vs Motor Speed

2.3.4 Sensor Location

Simulations of the magnetic field were performed to evaluate the potential locations for on-axis, in-plane, and off-axis alignments.

With a diametric magnet, the largest magnitude magnetic field vector at any air gap distance occurs when evaluating the field aligned to the polarization of the magnet. In this case, the first target location to examine is centered vertically with the magnet along a line directed radially outward from the center of the magnet.

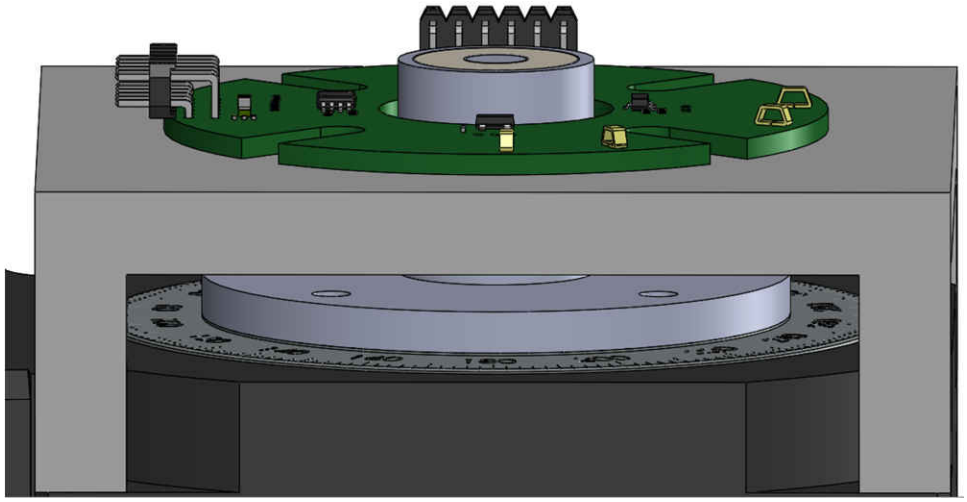

Figure 2-4. In-Plane Sensor Alignment

At this location, it is worthwhile to examine the peak magnetic flux density as well as the quality of the magnetic field for each component of the B-field over one full rotation. Figure 2-5 demonstrates the peak magnitude which is observed as the horizontal distance of the sensor changes as depicted in Figure 2-4.

Copyright © 2022 Texas Instruments Incorporated

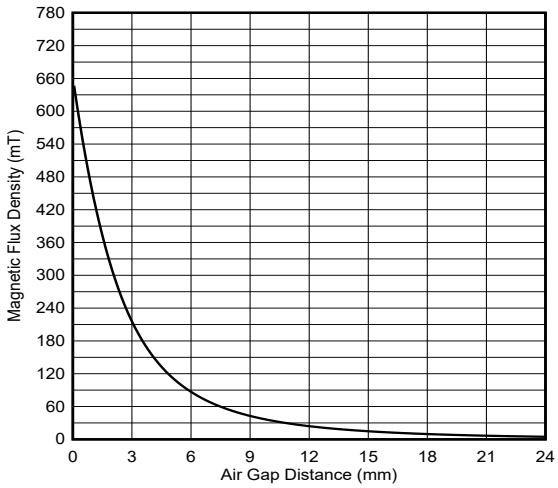

Figure 2-5. In-Plane Magnitude vs Airgap Distance

The subsequent plots depict the magnetic field vector components at a few select locations to demonstrate the nature of the magnetic field. In each case the sensor location is perfectly aligned with the center of the magnet, and therefore there is no Z component in the vector.

2-mm Airgap Magnetic Field Inputs is an example of a sensor placed too close to the magnet source. The input on the (X-axis) has a peak value of nearly 150 mT while the (Y-axis) input has a peak value over 300 mT, which exceeds the linear input range for TMAG5170.

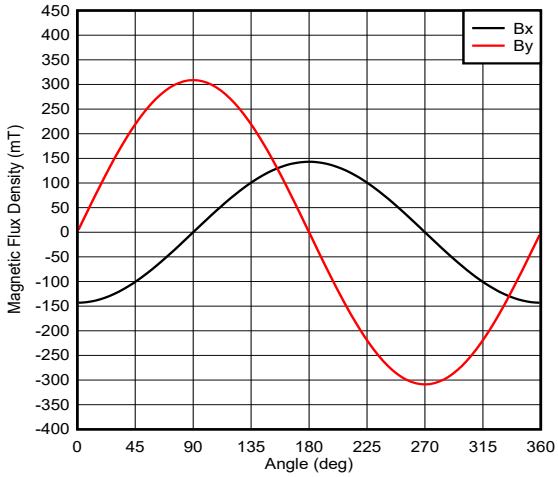

Figure 2-6. 2-mm Airgap Magnetic Field Inputs

Additionally, there is some minor harmonic distortion to the sinusoidal inputs. Ultimately any distortion to the magnetic field inputs results in some periodic angle error. For all magnets, the sinusoidal nature typically improves with range.

5.9-mm Airgap Magnetic Field Inputs shows a case where the field is too far from the sensor. While the X and Y components have an ideal sinusoidal form, the 4.5 mT peak input signal is too small to be used in high-precision applications. With such a small input signal, the output noise could cause significant errors in angle calculations.

Copyright © 2022 Texas Instruments Incorporated

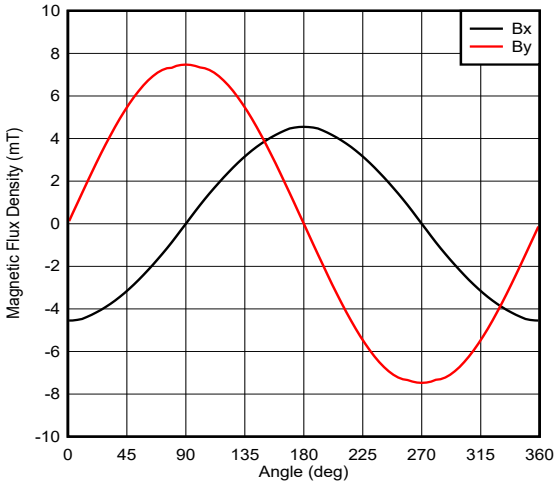

Figure 2-7. 20-mm Airgap Magnetic Field Inputs

The goal is to target an input near to the maximum of the linear magnetic sensing range of the target sensor. With target devices such as TMAG5170 and DRV5055, it is necessary to allow for system tolerances while selecting a sensor location to maximize SNR. Variations in device sensitivity, installation alignment, and magnet quality can all have an impact on the observed field magnitude.

Sensitivity options for these two devices are shown in Table 2-1.

Table 2-1. Linear Hall-Effect Sensor Input Ranges

DEVICE	LINEAR MAGNETIC SENSING RANGE (B_L)
TMAG5170A1	±25 mT , ±50 mT, ±100 mT
TMAG5170A2	±75 mT , ±150 mT, ±300 mT
DRV5055A1 DRV5055Z1	±22 mT
DRV5055A2, DRV5055Z2	±44mT
DRV5055A3, DRV5055Z3	±88 mT
DRV5055A4, DRV5055Z4	±176 mT

To allow for either device, a horizontal sensor range of 4.65 mm (DRV5055) and 5.9 mm (TMAG5170) from the magnet face were selected to ensure at all possible positions that the input field would be within the B_L of the TMAG5170A1 using the ±100 mT setting and DRV5055A4.

At this range, the expected input magnetic field components are shown in 5.9-mm Airgap Magnetic Field Inputs.

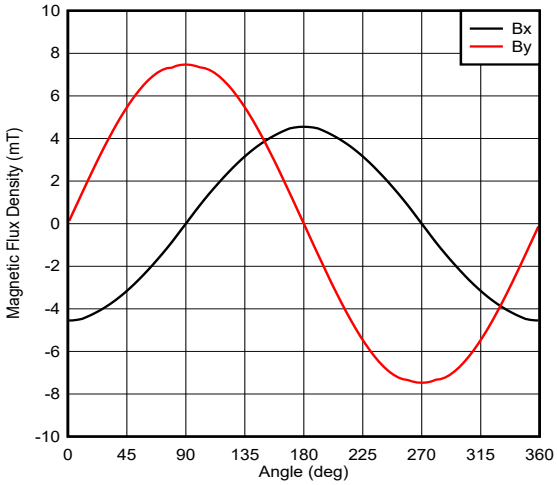

Figure 2-8. 5.9-mm Airgap Magnetic Field Inputs

Copyright © 2022 Texas Instruments Incorporated

It is evident that the sensor inputs at this range are appropriate for TMAG5170, but there is significant amplitude mismatch between the X and Y axes. If these inputs were used directly, the resulting angle calculation would effectively map an elliptical input. The arctangent is a circular function, and so this contributes significant measurement error if not corrected. Mapping the X and Y magnitudes into a coordinate plane reveals this relationship.

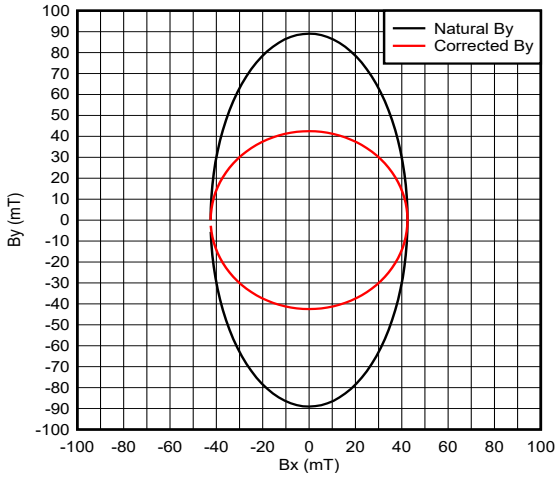

Figure 2-9. Benefit of Amplitude Matching in Angle Calculations

The effective angle error is significant. To counter this effect, attenuate the (X-axis) results or the (Y-axis) result requires a gain increase. Either transformation results in normalization of the inputs for the angle calculation and resolves this error to the expected circular format.

5.9-mm Airgap Magnetic Field Inputs shows that the in-plane alignment is not ideal for DRV5055 in the SOT-23 package option due to the directionality of the magnetic field vector. When perfectly coplanar to the center of the rotating magnet, there is no vertical component. If using the SOT-23 package option for this device, the sensor detects the Z-component of the field vector which in this alignment is 0 mT for all angles. Instead, it is more ideal to use the LPG through-hole package in this location. TIDA-060040 includes an optional component footprint for this package variant adjacent to the target location for the SOT-23 package. Make sure the sensors have the same vertical spacing from the PCB to ensure each observes an equivalent input from the rotating magnet, and that the sensor is installed orthogonal to the surface of the PCB. If using the DRV5055 solution, remove the unused package option to allow for a more ideal PCB layout.

Copyright © 2022 Texas Instruments Incorporated

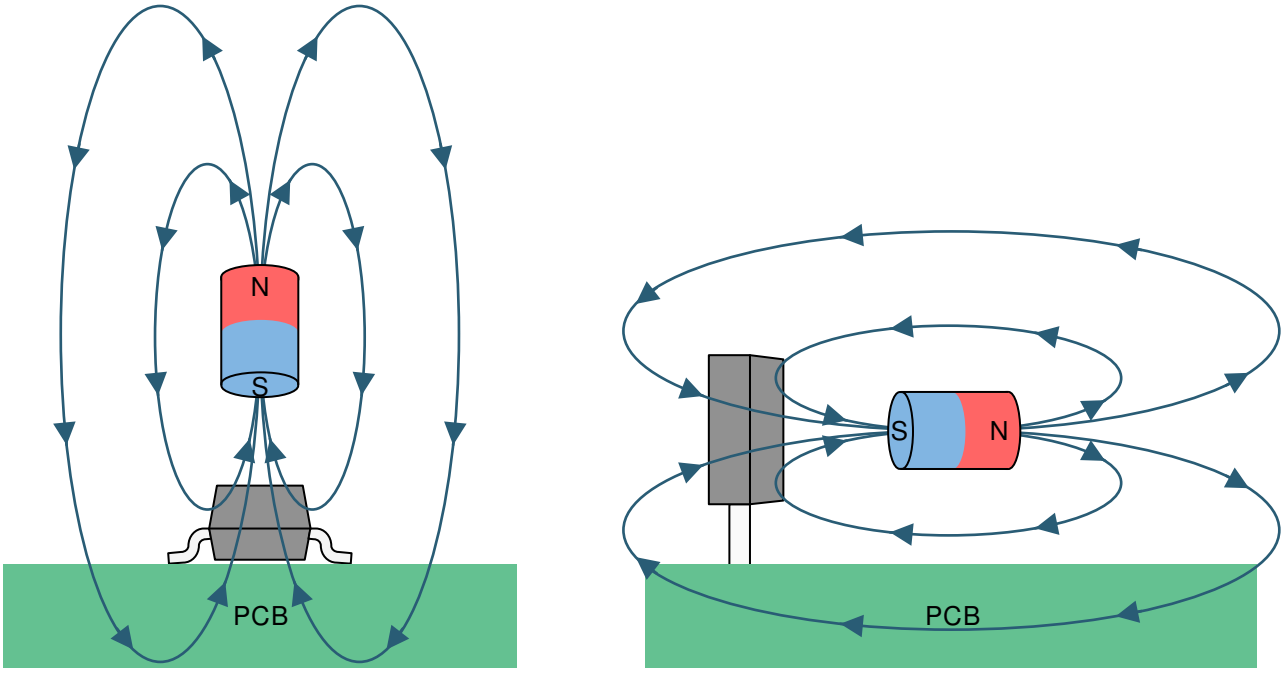

Figure 2-10. DRV5055 Sensitivity

An alternative to setting tight controls for the mechanical assembly using the TO-92 package is to provide vertical offset for the sensor location which results with a component of the magnetic field vector directed vertically.

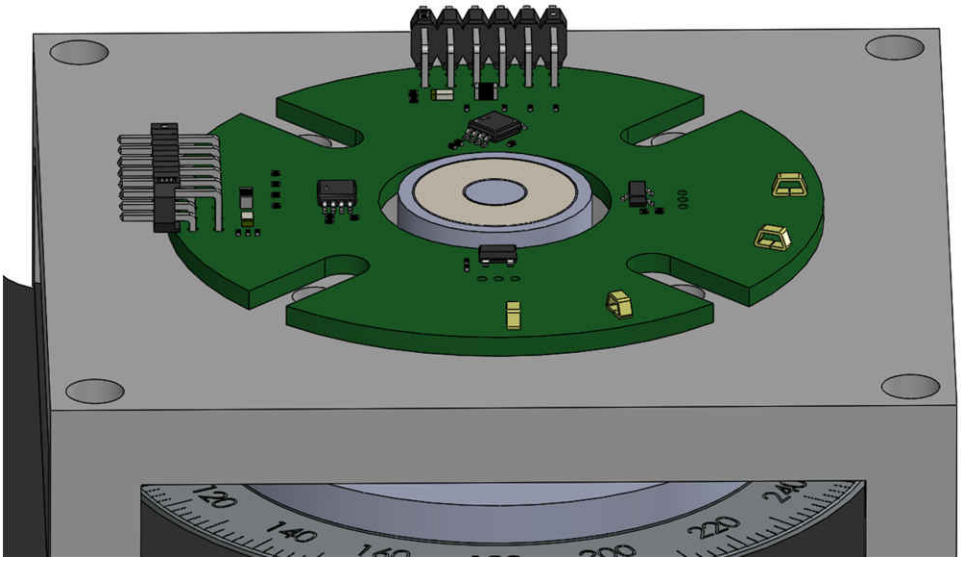

Figure 2-11. Off-Axis Sensor Alignment

The result is an alignment which is no longer coplanar to the magnet center. This placement is referred to as off-axis (or out-of-plane). In effect, all placements which are not coplanar to the magnet or centered on the axis of rotation fall into this category. The key characteristic is that the magnetic field vector has a sinusoidal component in all three axes. As a result, there is a wide range of locations suitable for the SOT-23 package option.

Copyright © 2022 Texas Instruments Incorporated

Off-Axis Sensor Alignment shows a sensor location where the only change from the in-plane sensor alignment is a vertical offset of 3.175 mm. This results with the same horizontal alignment from the magnet face, and the sensor is now coplanar to the upmost face of the magnet. In this location the magnitude of each field component is shown in Off-Axis Magnetic Field Inputs.

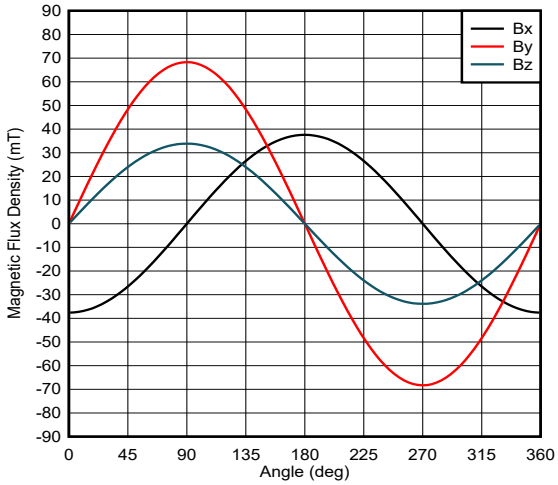

Figure 2-12. Off-Axis Magnetic Field Inputs

Depending on the vertical placement, the magnitude of each field component may vary, and use of a 3D sensor allows for selection of the two axes which provide the best quality inputs.

Aside from the off-axis and in-plane positions, the final alignment to examine is the on-axis placement.

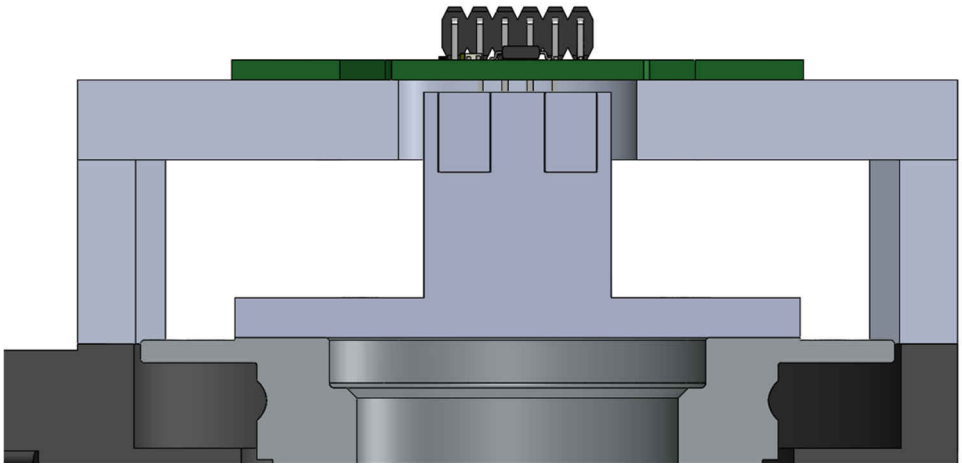

Figure 2-13. On-Axis Sensor Alignment

This is a unique location where the magnetic field vector is inherently parallel to the circular face of the magnet. This condition is ideal for 3D sensors, such as TMAG5170. Since the vector is entirely within the XY plane, a single sensor should experience perfectly sinusoidal inputs when monitoring these axes.

Copyright © 2022 Texas Instruments Incorporated

On-Axis Magnetic Field Inputs shows the sensor inputs at a range of 3 mm above the magnet.

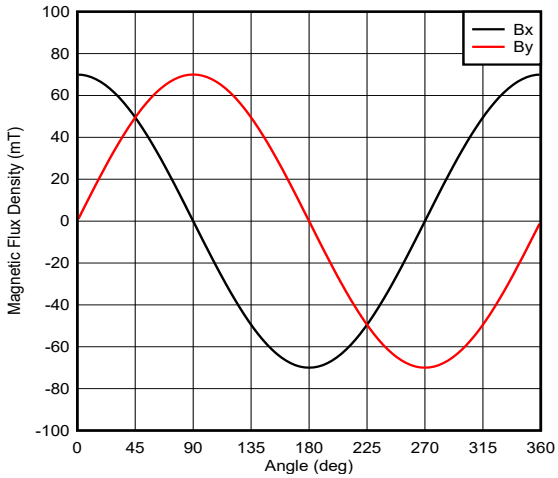

Figure 2-14. On-Axis Magnetic Field Inputs

2.3.5 Expected Performance

Based on the simulation results in Figure 2-15, Figure 2-16, and Figure 2-17, it is now possible to estimate any angle error resulting from amplitude mismatch or non-sinusoidal inputs.

- TMAG5170 Error

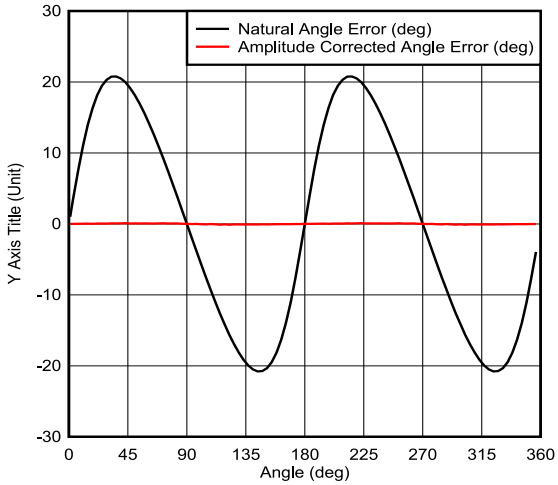

Figure 2-15. Expected TMAG5170 In-Plane Angle Error

Copyright © 2022 Texas Instruments Incorporated

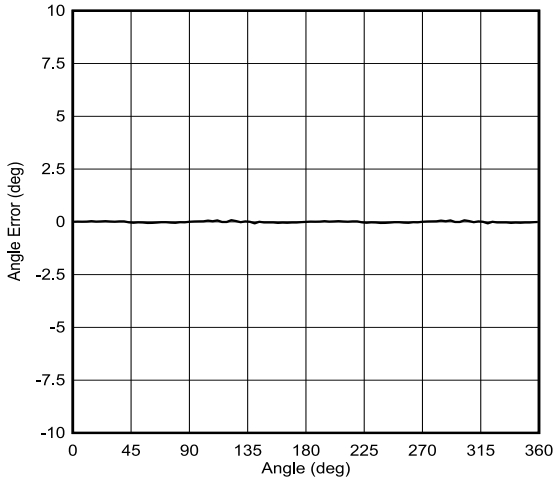

Figure 2-16. Expected TMAG5170 Off-Axis Angle Error

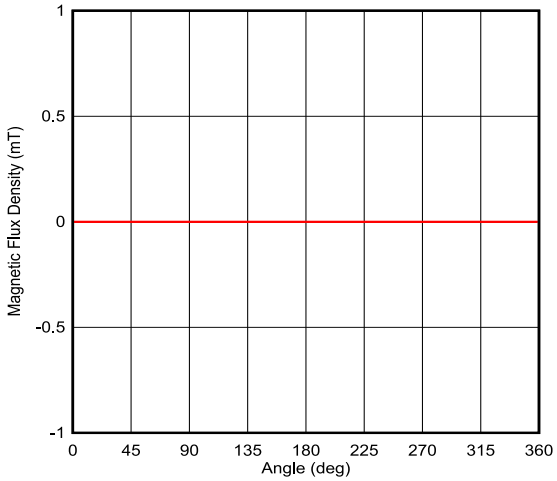

Figure 2-17. Expected TMAG5170 On-Axis Angle Error

- DRV5055 Error

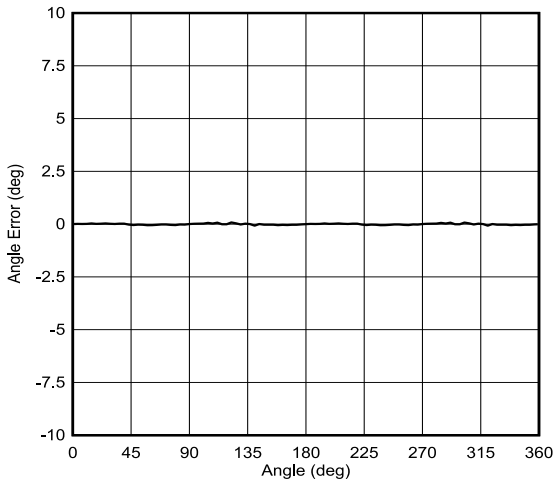

Figure 2-18. Expected DRV5055 Off-Axis Angle Error

What is evident from each scenario, is that with amplitude correction, each option provides a viable path to design angle encoding. However, each of these cases has assumed ideal mechanical tolerances. Test Results details the actual observed error from each of these device configurations.

Copyright © 2022 Texas Instruments Incorporated

Regardless of the option, input referred noise also impacts overall angle accuracy. As the input SNR ratio varies, the resulting peak noise induced angle error approximately follows the trend in Noise Induced Angle Error. For any sensor used, the required input signal can be calculated based on the angle accuracy requirement.

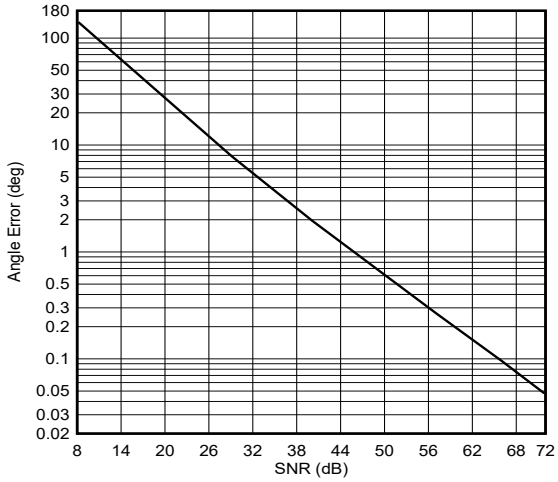

Figure 2-19. Noise Induced Angle Error

2.3.6 Layout for Sensor Location

One important factor when designing an angle encoder using these devices is the actual sensor location on the PCB. The sensor placement in the package may result with unintentional placement errors in any of the 3 axes.

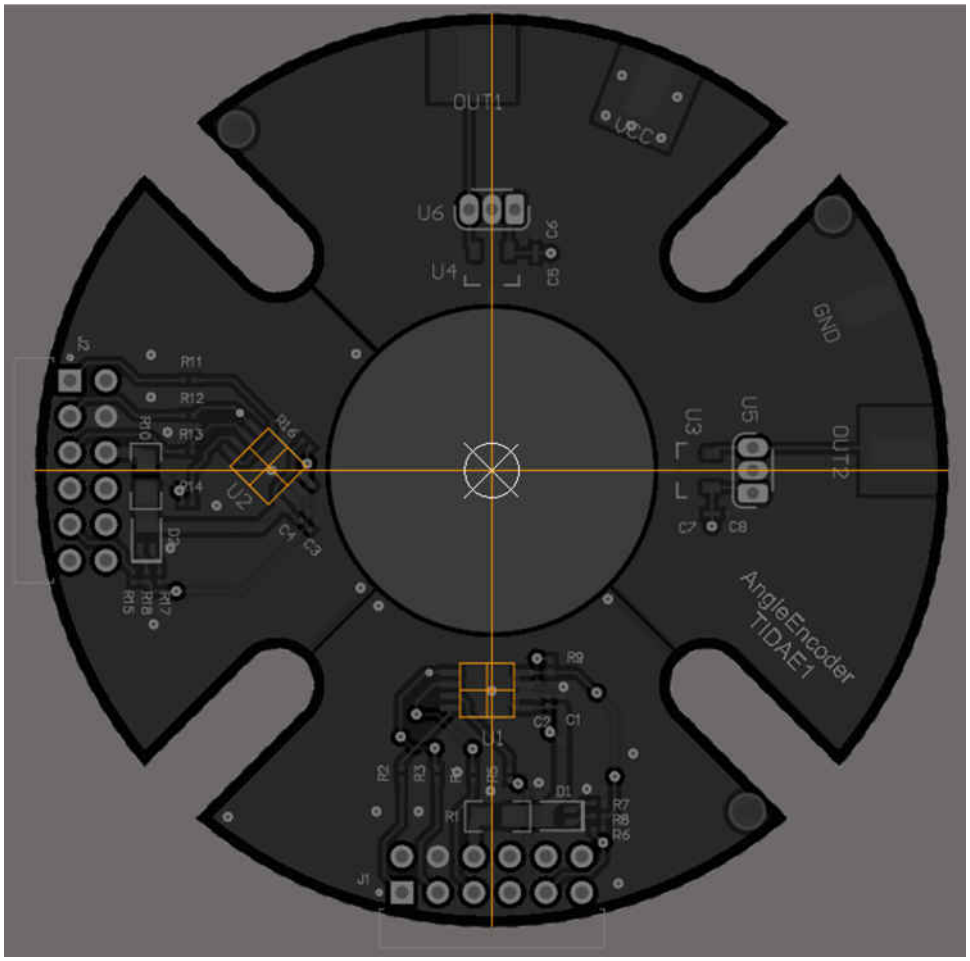

Figure 2-20. TIDA-060040 Sensor Placement

Copyright © 2022 Texas Instruments Incorporated

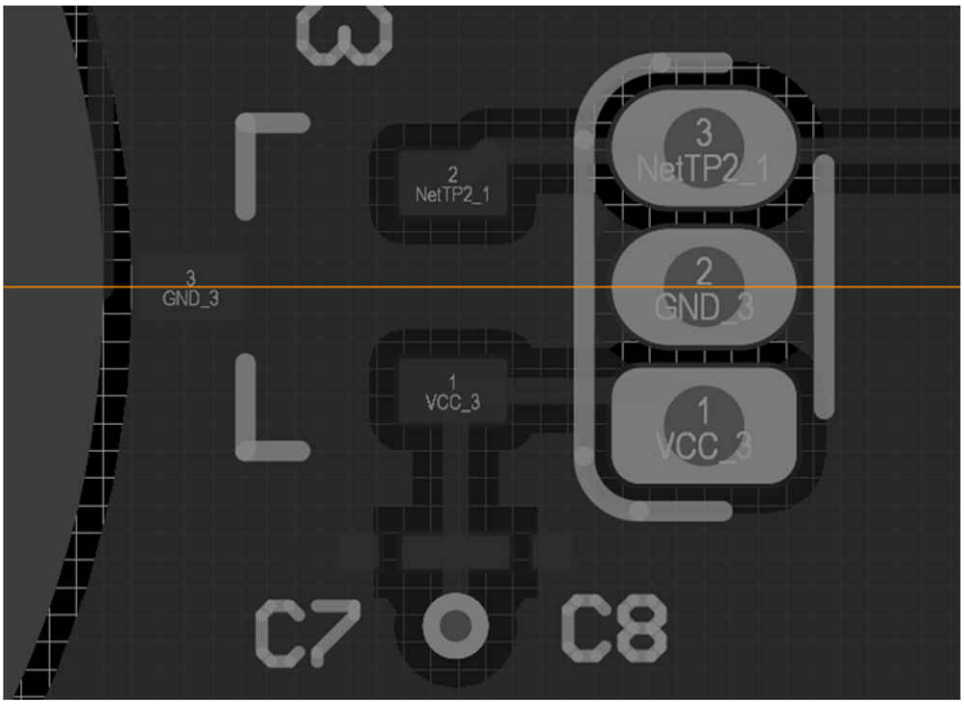

Figure 2-21. DRV5055 Sensor Location

DRV5055 has the benefit that the sensor location in the XY plane is centered relative to the package. However, the implementation for this device requires two sensors placed 90° separated about the magnet. Additionally, it may be necessary to use an LPG through-hole package depending on the sensor location.

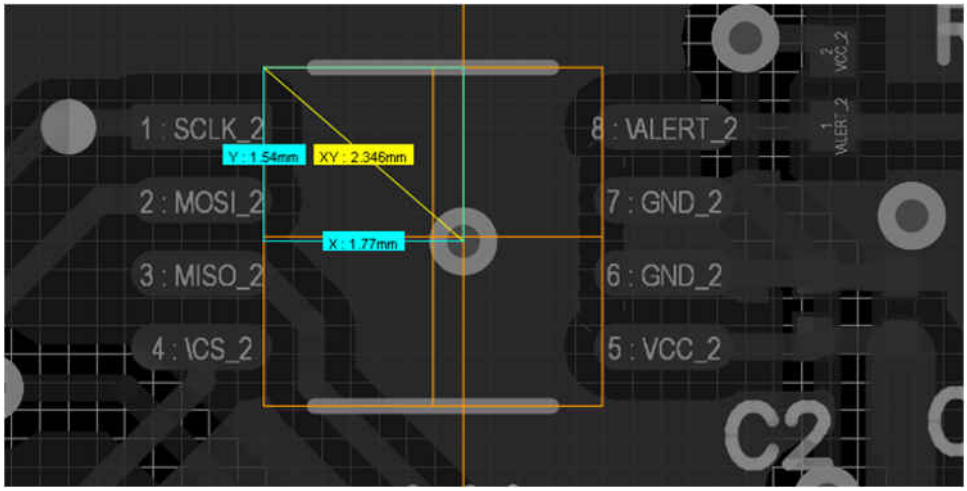

Figure 2-22. TMAG5170 Sensor Location

For TMAG5170, the layout files TIDA-060040 contain an alignment layer which indicates the actual sensor location. Additionally, a via has been placed at the target sensor location to assist with alignment.

Copyright © 2022 Texas Instruments Incorporated

2.3.7 45° Alignment

The TIDA-060040 also shows an additional alignment option for TMAG5170.

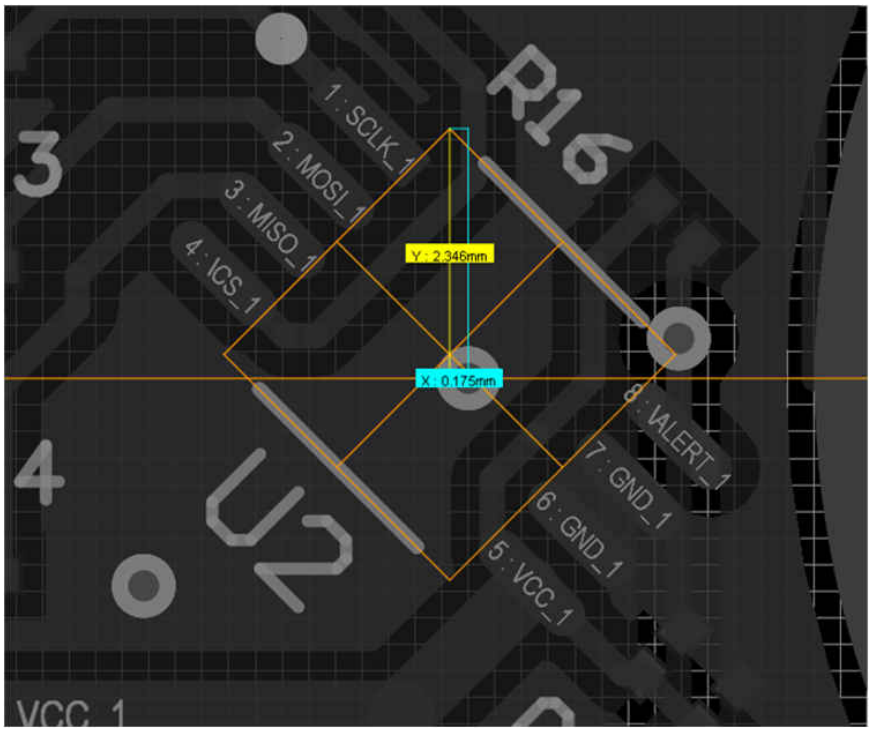

Figure 2-23. TMAG5170 45° Alignment

This second sensor location option has the device physically rotated 45°. Instead of the normal orthogonal alignment, the X and Y axes of the sensor each observe the same input magnitude. The effective input for each axis is the average of the two axes. The benefit of installing the device with this rotation is that it allows the sensor to be placed in locations where one input might be excessively large, one input might not have sufficient SNR, or both. This alignment offers a potentially more compact solution, but at the cost of phase alignment. By rotating the sensor in this fashion, a phase error is introduced which is a function of the total mismatch between the two channels. This phase error is depicted as β in Equation 5. To properly use inputs with a phase error, the following trigonometric adjustment to the arctangent calculation is helpful:

$$Acos(\theta - \beta) = Acos(\theta)\cos(\beta) + A\sin(\theta)\sin(\beta) \tag{5}$$

$$\frac{In_2}{In_1} = \frac{A\cos(\beta)\cos(\theta) + A\sin(\theta)\sin(\beta)}{A\sin(\theta)} \tag{6}$$

$$\frac{In_2}{In_1} = \frac{\cos(\beta)}{\tan(\theta)} + \sin(\beta) \tag{7}$$

$$\tan(\theta) = \frac{\cos(\beta)}{\left(\frac{In_2}{In_1} - \sin(\beta)\right)} \tag{8}$$

$$\theta = \tan^{-1}\left(\frac{\cos(\beta)}{\left(\frac{In_2}{In_1} - \sin(\beta)\right)}\right) \tag{9}$$

When applying Equation 9, it is important to verify the actual phase shift of the vector components. Manufacturing alignment errors and the combination of unequal amplitude inputs may result in a value of β which differs from the physical rotation of the sensor.

Copyright © 2022 Texas Instruments Incorporated

3 Hardware, Software, Testing Requirements, and Test Results

3.1 Hardware Requirements

Figure 3-1 illustrates the schematic and board connections of TIDA-060040.

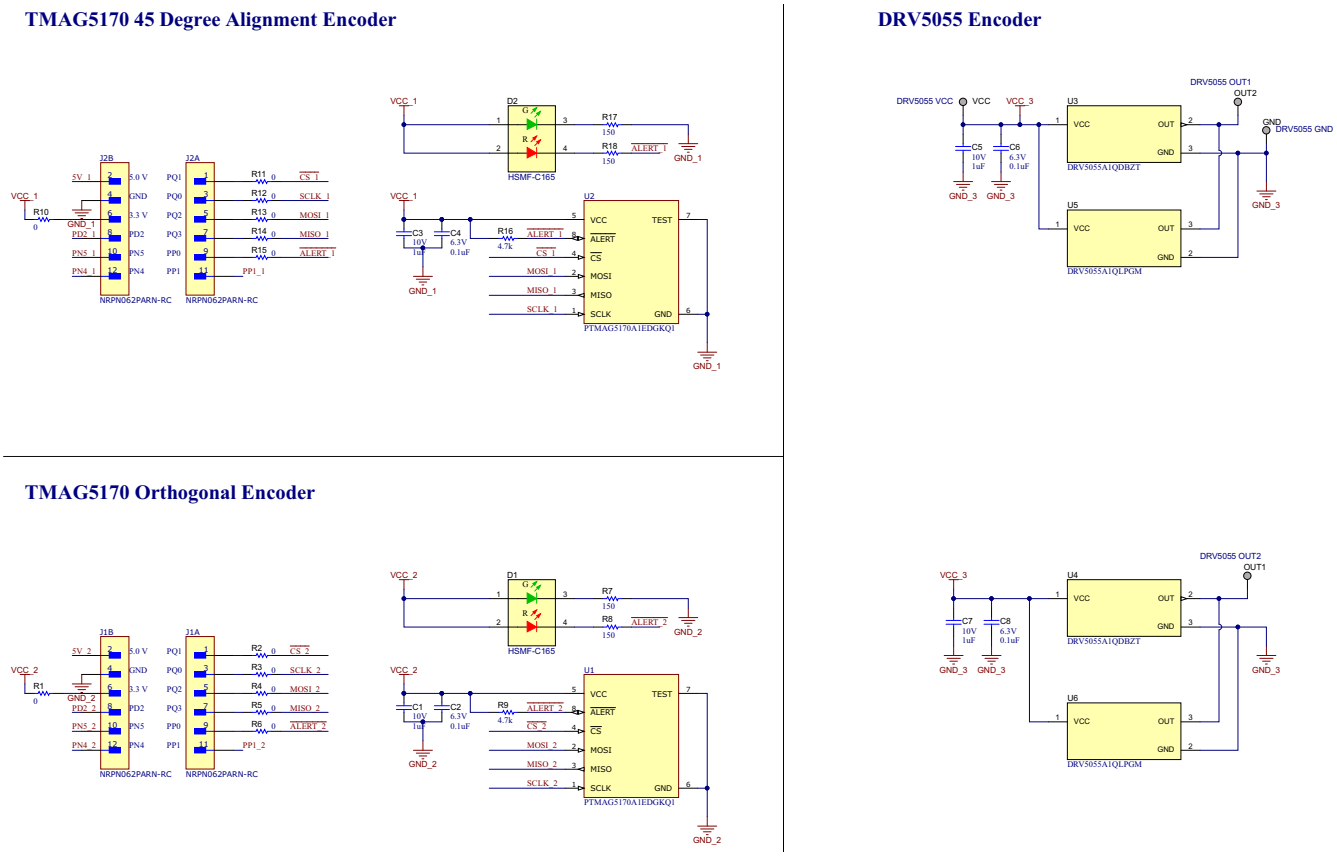

Figure 3-1. TIDA-060040 Schematic

The J1 and J2 board connector was configured for compatibility with TI-SCB (SENS077).

Table 3-1. J1 and J2 Pin Connection Summary

PIN	SIGNAL
1	nCS
2	Not Used
3	SCLK
4	GND
5	Controller Out Peripheral In
6	3.3 V
7	Controller In Peripheral Out
8	Not Used
9	Alert
10	Not Used
11	Not Used
12	Not Used

Copyright © 2022 Texas Instruments Incorporated

Figure 3-2 shows the layout of TIDA-060040.

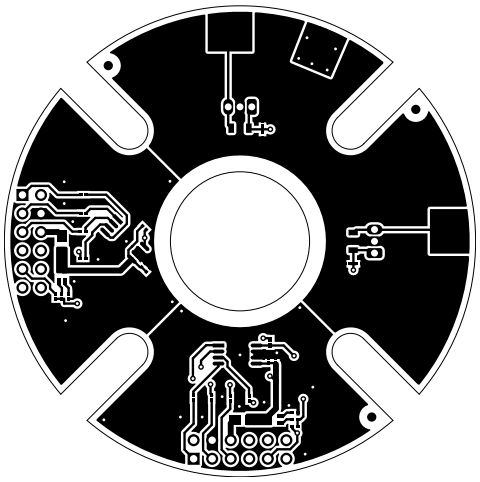

Figure 3-2. TIDA-060040 Layout

This layout may be used or adjusted as needed to suit any magnet and motor geometry. While this design includes options for TMAG5170 orthogonal, TMAG5170 at 45° rotation, and DRV5055, it is likewise possible to reduce the PCB layout for a single sensor option as desired.

Copyright © 2022 Texas Instruments Incorporated

3.2 Test Setup

3.2.1 Test Equipment

The design was tested using the following hardware:

- Newport Motion Controller (ESP301)
- Newport Motorized Rotation Stage (URS50BCC)
- Magnet (R834DIA)
- 3D printed magnet holder

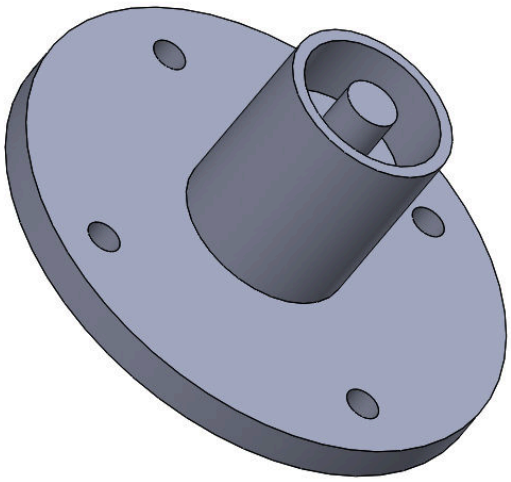

Figure 3-3. Holder

- 3D printed mounting plate

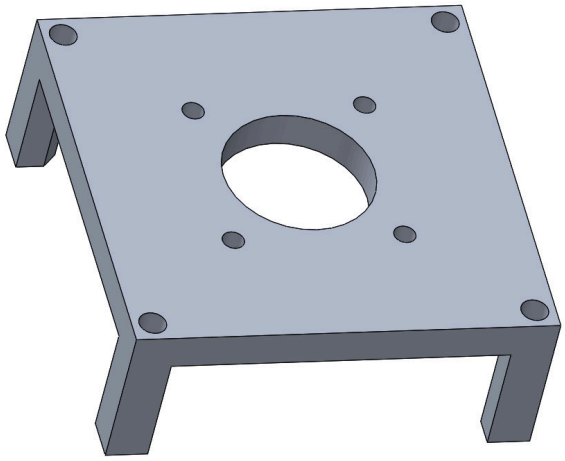

Figure 3-4. Mounting Plate

- TI-SCB (SENS077)
- Micro USB cable

Copyright © 2022 Texas Instruments Incorporated

3.2.2 Test Hardware Configuration

1. Connect Newport rotation stage to the Newport motion controller
2. Mount 3D printed magnet holder to the Newport rotation stage
3. Insert magnet into recess in magnet holder
4. Connect TIDA-060040 to the 3D printed mounting plate
5. Connect TIDA-060040 to the TI-SCB (TI sensor control board)
6. Connect TI-SCB to PC via USB cable

3.2.3 Test Software Configuration and Initial Data Capture

1. Launch TMAG5170UEVM GUI
   a. Verify connectivity to TMAG5170A1 sensor
      i. Refer to TMAG5170UEVM User's Guide for steps to debug the connection to the sensor control board
   b. Configure TMAG5170A1
      i. Set TMAG5170A1 to the ±100 mT input range for all axes
         • The channel sensitivity can be set lower as long as the inputs do not reach saturation, but should match between the two axes used for angle calculations.
      ii. Set TMAG5170A1 to *Active Measure Mode*
      iii. Set *Averaging* at 32x and conversion pattern to XYZZYX
         • The *Newport Rotation Stage* has a maximum speed limitation of 20 seconds/rev.
      iv. Set GUI to collect data continuously for a period greater of 1 or more full revolutions
         • Capture peak data for X, Y, and Z channels
2. Using captured data it is possible to perform first-order calibration of the system.
   a. Based on X, Y, and Z channel outputs, select inputs to require the least sensitivity gain correction.
      i. TMAG5170 is capable of an 11-bit gain correction with a multiplication factor ranging from 0 to 2.
      ii. Scale up a channel where possible, or to use the minimum attenuation needed to achieve equally matched amplitude from two sinusoidal input channels.
   b. Analyzing peak-to-peak output levels, it is also possible to calculate and offset correction to remove and DC bias resulting from signal chain errors or external conditions.
   c. Apply the sensitivity gain and offset corrections and verify results over one full rotation. The measured amplitude for each axis should be identical. It is also possible to now disable any axis which is not required for angle calculations.
3. The system should now have device related errors removed and inputs which are matched for angle calculation. Errors related to mechanical alignment may still be present, capture rotation data to remove these errors. This process is detailed in the Test Results section.

Copyright © 2022 Texas Instruments Incorporated

3.3 Test Results

The TIDA-060040 was tested in each of the three orientations discussed previously: On-axis, In-Plane, and Off-Axis. The results from each orientation were then calibrated and a final error using controller calculations and the internal CORDIC output are shown at angle steps of 0.25° for one full rotation.

3.3.1 Calibration Methods

After removing signal chain errors from the calculation, there are still several possible mechanical sources that may impact the quality of the input magnetic field used to calculate angle:

- **Motor Shaft tilt** – results in an orthogonality error between TIDA-060040 and the rotating magnet. This produces a fixed shift to the expected field alignment.
- **Motor Shaft offset** – results with the sensor in a different location and orientation than targeted. Depending on the offset direction this can influence either peak input amplitude to or phase alignment of the inputs.
- **Magnet tilt** – results when the magnet is not installed orthogonally to the shaft rotation axis. The magnet appears to wobble during rotation and produces a changing field orientation.
- **Magnet and Shaft Eccentricity** – results from either the axis of rotation not aligning to the center of the shaft or the magnet not having its center aligned to the axis of rotation. This produces a lateral change of position during rotation which impacts the B-field magnitude.
- **Soldering and assembly alignment errors** – Errors resulting from package alignment during solder-reflow to tolerances when mounting the TIDA-060040 PCB may result in various orientation and position errors that may similarly impact the phase and magnitude of the inputs
- **Near field behavior** – At close proximity to many magnet types, the magnetic field may produce a non-ideal input for the sensor. The target input field is a purely sinusoidal waveform. The observed field when a sensor is placed very close to a magnet will typically take on some degree of distortion which is dependent on the magnet geometry.

All of the preceding errors combine to create non-linearity in the angle measurement. While these factors are not predictable, they may combine to create a substantial error which, if unaccounted for, results with poor system control. Given these factors it is necessary to implement a final calibration to resolve the resulting error for the highest precision control.

Multi-point linearization is one useful approach and may be used to quickly adapt to system-to-system variations. Consider the hypothetical error in Cyclical Angle Error.

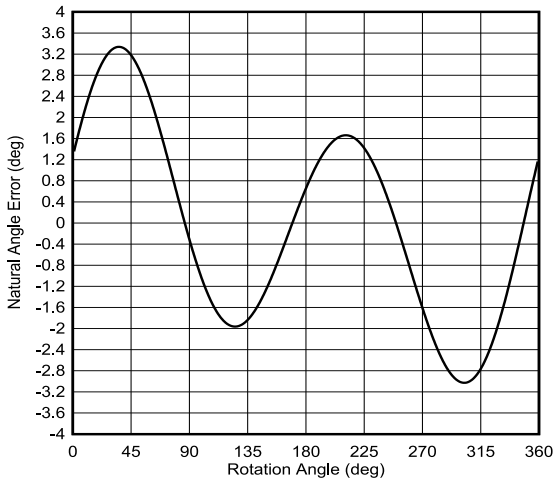

Figure 3-5. Cyclical Angle Error

In this example, a multi-point linearization captures the absolute error at any number of discrete points. The controller then assumes a linear estimation of error between those points. As the number of points increases, the accuracy of the estimation approaches the real error. When an approximation of the error for any given angle is determined, it may then be directly subtracted from the measured angle.

Copyright © 2022 Texas Instruments Incorporated

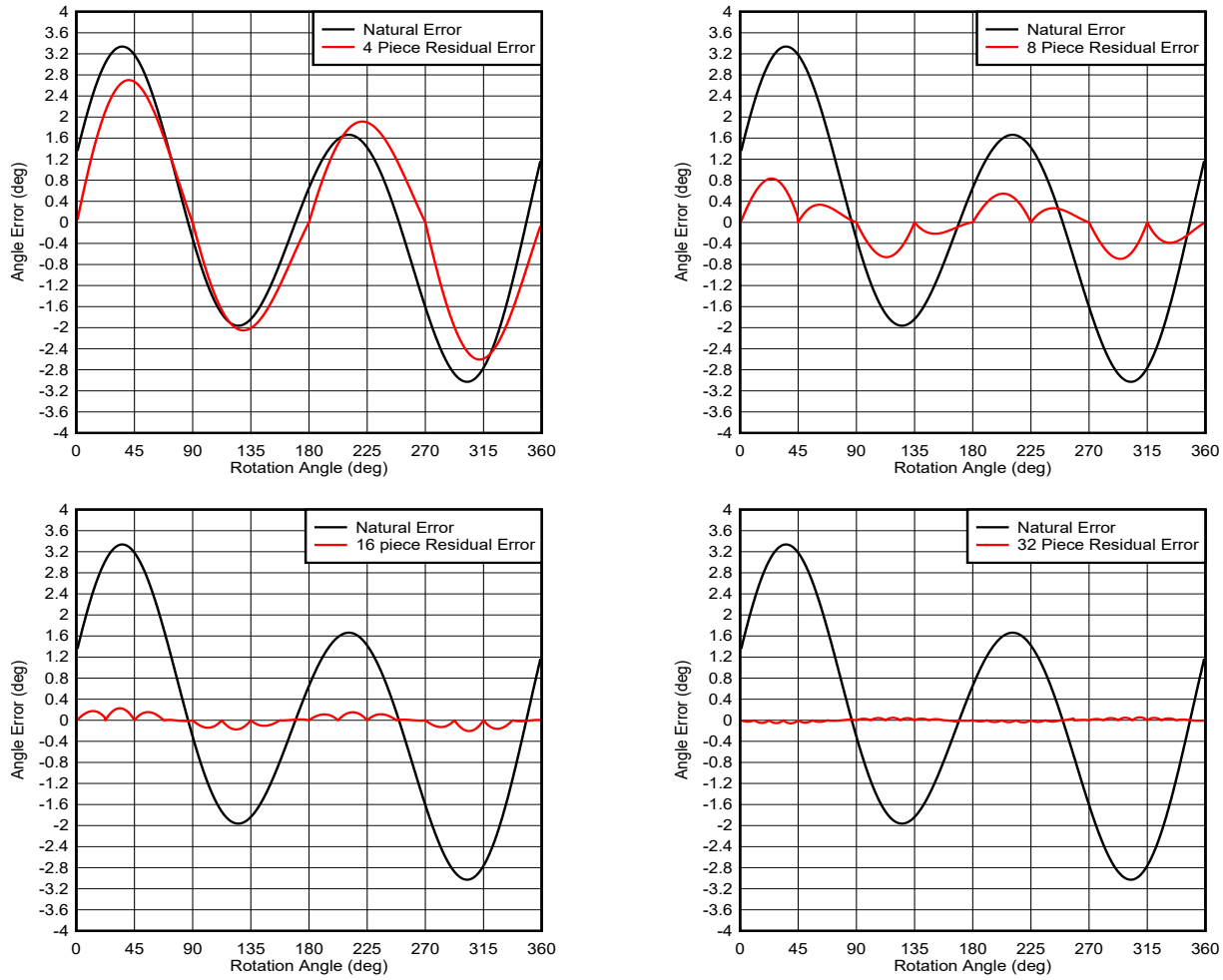

Figure 3-6. Multi-Point Linearization

As the number of samples increases, the resulting peak error is continually reduced. Depending on the required system accuracy, 8 points to 64 points can often provide adequate accuracy. In a more advanced approach, it is possible to match the error profile to a set of equations which are a combination of harmonics of the rotation frequency. By performing complex analysis, it is possible to generate a series of coefficients, α_i and β_i, that may be used as shown in Equation 10:

$$Correction\ Factor = \sum_{i=1}^{n} [\alpha_i \sin(i*\theta) + \beta_i \cos(i*\theta)] \quad (10)$$

Here, the total error is a combination of the scalar factors for each harmonic of the measured angle. Using this approach can produce superior results to the multi-point linearization method and does not require storing as much data in memory.

Copyright © 2022 Texas Instruments Incorporated

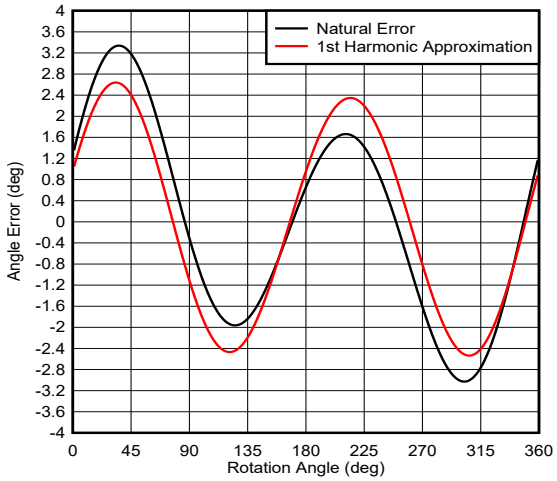

Figure 3-7. First Harmonic Approximation

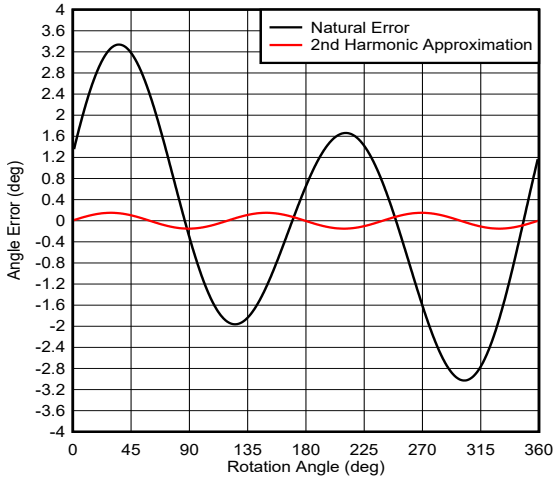

Figure 3-8. Second Harmonic Approximation

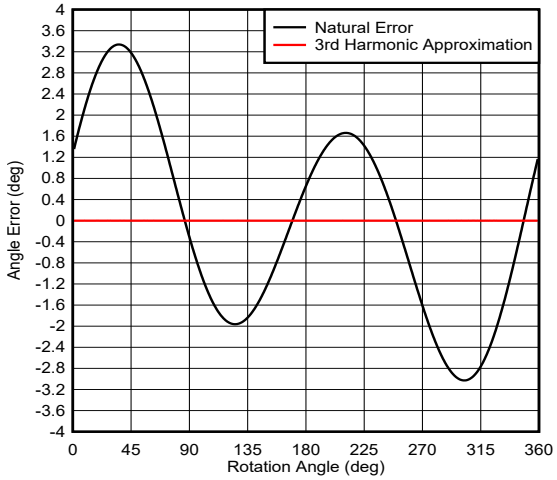

Figure 3-9. Third Harmonic Approximation

For all of the test results, the data was captured at 0.25° intervals and analyzed for harmonic reduction.

To achieve consistent results in a real manufacturing environment, some degree of calibration for each system is likely necessary as each unit would exhibit slight variations in the various mechanical tolerances.

Copyright © 2022 Texas Instruments Incorporated

3.3.2 TMAG5170 On-Axis

The on-axis alignment is the ideal case for measuring the angle of a magnetic field but requires additional area about the motor. Either the motor must be dual shaft or the end of the shaft is not available to drive the load. This results in the least compact solution size when implemented with any given motor. The impact of mechanical error is minimized in this orientation; however, which results in best uncalibrated results.

The mounting plate was configured to match the simulation results shown in Sensor Location.

Note

Mechanical errors detailed in Calibration Methods are all present to some degree in each test case and the captured data reflects the result of these conditions after amplitude and offset corrections were applied.

The manual assembly and manufacturing tolerances of the entire setup resulted with mechanical errors which must be addressed. These alignment flaws demonstrated in the test results are crucial for the purpose of demonstrating the significance of alignment errors and how the calibration process can correct even large scale angle error. Strictly controlled manufacturing practices results with a reduced error from what is depicted for each case.

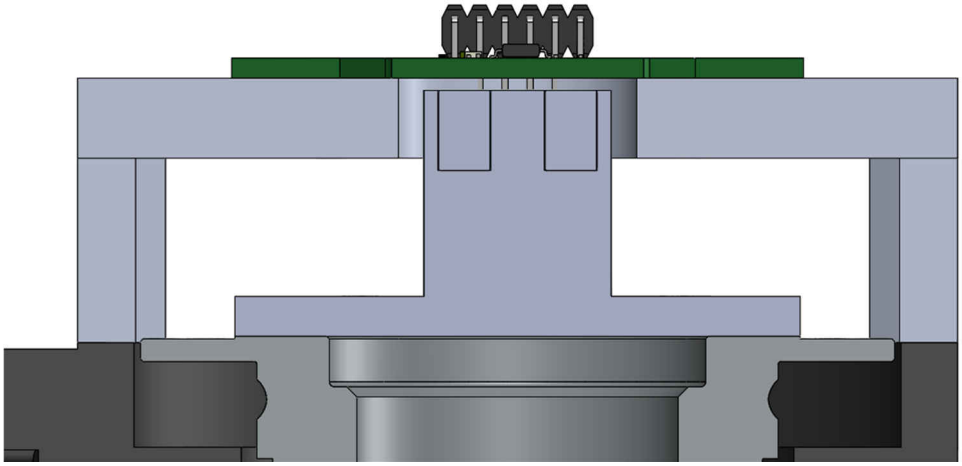

Figure 3-10. On-Axis Configuration

On-Axis Mechanical Angle Error shows the resulting pre-calibrated error captured for this alignment.

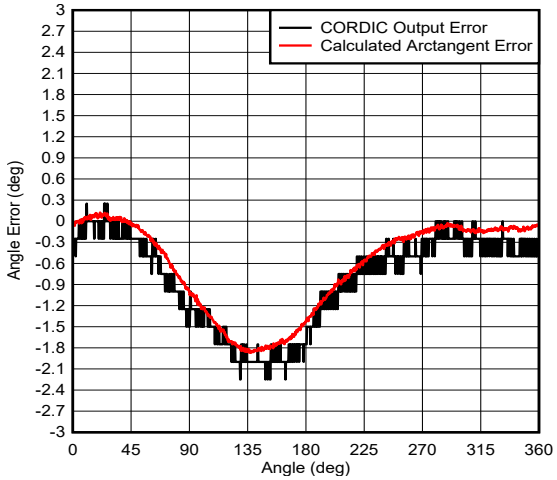

Figure 3-11. On-Axis Mechanical Angle Error

Copyright © 2022 Texas Instruments Incorporated

Of all the alignment cases, on-axis is the most forgiving of mechanical alignment errors. Overall the field vector remains nearly parallel to the face of the magnet and therefore magnitude and phase shifts at the input are not as significant as is seen with the other alignment cases.

Table 3-2. On-Axis Harmonic Correction Factors

HARMONIC	α_i	β_i
1	0.42	–0.73
2	–0.35	0.07
3	–0.01	0.06
4	–0.02	0.01

On-Axis Calibrated Angle Error shows the resulting error for both a direct arctangent calculation and for the CORDIC output after applying the harmonic data.

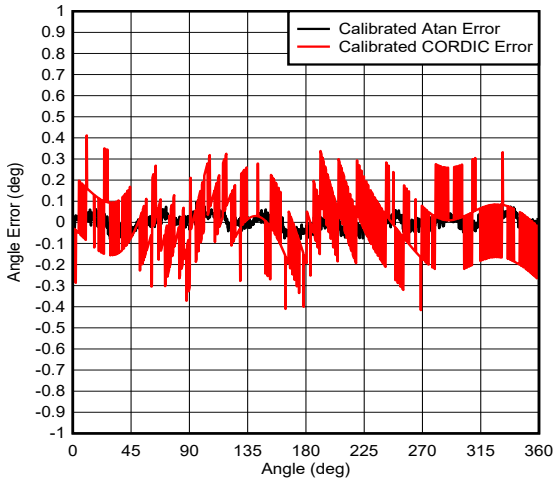

Figure 3-12. On-Axis Calibrated Angle Error

It is worth noting here that the 0.25° resolution of the TMAG5170 CORDIC output does limit the measurement accuracy. To achieve the highest accuracy, directly calculate the arctangent result from the X and Y component outputs of the device. The benefit of the CORDIC output of TMAG5170 is that it reduces the burden for the microprocessor and can reduce overall measurement latency.

3.3.3 TMAG5170 In-Plane

The in-plane alignment differs from the on-axis approach in that the sensor is placed coplanar to the magnet. This produces the smallest profile solution overall, but produces highly imbalanced input magnitudes.

Additionally, this alignment is the most susceptible to mechanical errors which is evident when examining the peak angle error. This position is very sensitive to eccentricity errors in the magnet rotation. Any magnet centering misalignment results with a changing airgap range. As demonstrated in In-Plane Magnitude vs Airgap Distance, small variations at this range have a significant impact on the magnitude of the magnetic field. It is particularly important when configuring a sensor in this position to exercise a great deal of care to achieve an exact mount for the magnet.

Additionally, at the outer edge of the magnet, the field vector direction is constantly changing as it wraps around to the opposing magnet pole. As a result tilt and alignment errors will result in phase error and changing input amplitudes.

Copyright © 2022 Texas Instruments Incorporated

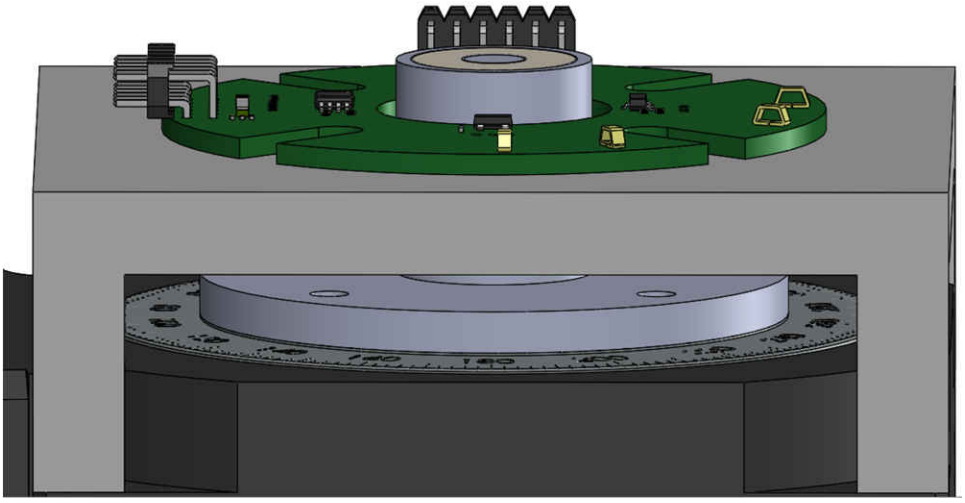

Figure 3-13. In-Plane Configuration

In-Plane Mechanical Angle Error shows the resulting pre-calibrated error captured for this alignment.

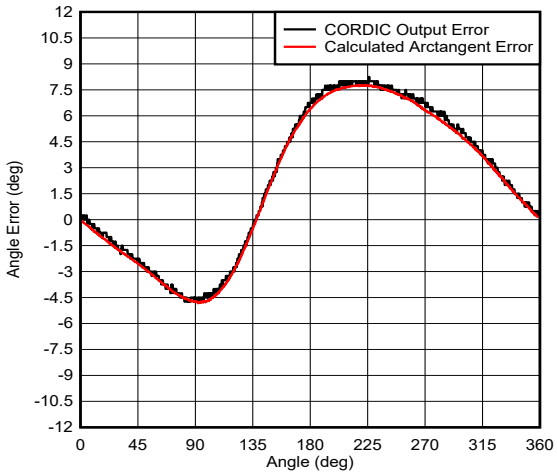

Figure 3-14. In-Plane Mechanical Angle Error

The angle error shown for the in-plane alignment appears quite extreme. With the assembly alignment errors for this test setup, a very dramatic angle error resulted. Even with this extreme of an error, it is still possible to apply a calibration to the end result to achieve accuracy below 0.1°.

Table 3-3. In-Plane Harmonic Correction Factors

HARMONIC	α_i	β_i
1	5.33	2.68
2	–0.5	–1.22
3	–0.26	0.51
4	0.17	0.05
5	–0.04	–0.02

Copyright © 2022 Texas Instruments Incorporated

In-Plane Calibrated Angle Error shows the resulting error for both a direct arctangent calculation and for the CORDIC output after applying the harmonic data.

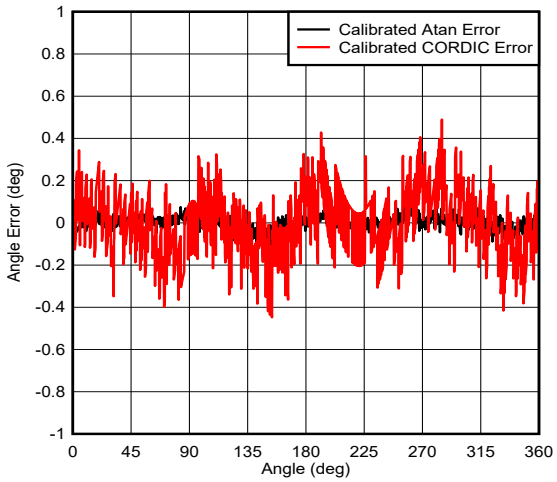

Figure 3-15. In-Plane Calibrated Angle Error

3.3.4 TMAG5170 Off-Axis

A third option represents every other possible location about the magnet. While the expected inputs for on-axis and in-plane were purely two dimensional, it is normal for the off-axis case to have field components in all three directions.

With the versatility of TMAG5170 to detect 3D fields, it is possible to use various sensor orientations and use any two vector components which are 90° out of phase. In this case XZ field components were used to calculate angular position.

The observed error for this alignment were similar to what was observed with the In-Plane Configuration.

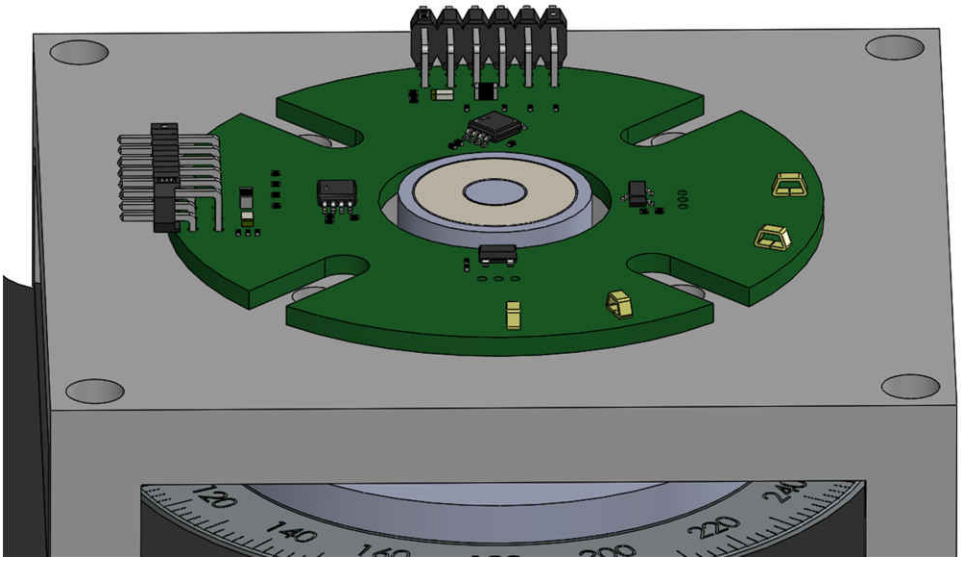

Figure 3-16. Off-Axis Configuration

Copyright © 2022 Texas Instruments Incorporated

Off-Axis Mechanical Angle Error shows the resulting error for both a direct arctangent calculation and for the CORDIC output after applying the harmonic data.

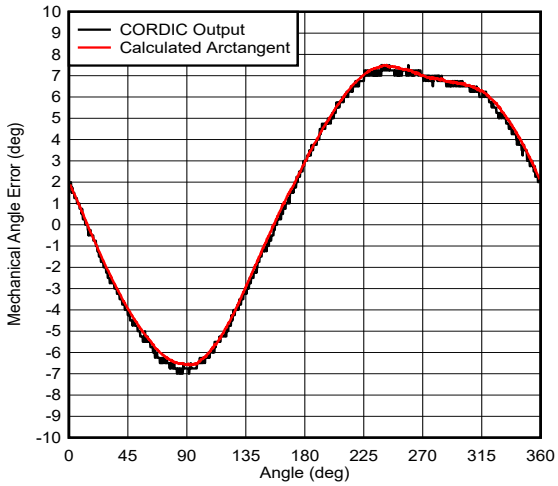

Figure 3-17. Off-Axis Mechanical Angle Error

Table 3-4. Off-Axis Harmonic Correction Factors

HARMONIC	α_i	β_i
1	–6.97	–0.55
2	–0.05	1.12
3	–0.15	0.07
4	–0.13	–0.13
5	0.02	0.03

Off-Axis Calibrated Angle Error shows the resulting error after applying the harmonic data.

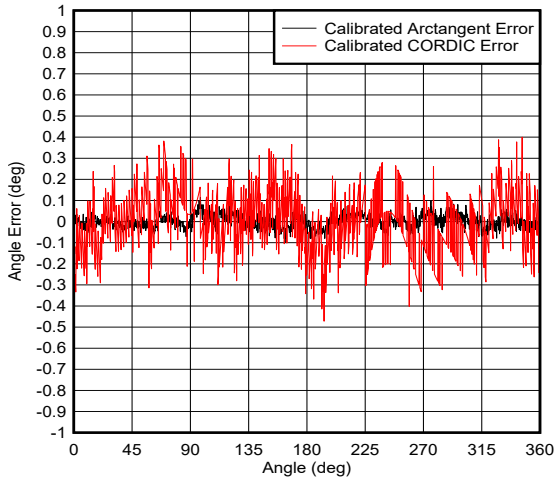

Figure 3-18. Off-Axis Calibrated Angle Error

Copyright © 2022 Texas Instruments Incorporated

3.3.5 TMAG5170 45° Alignment

As discussed in Design Considerations, the 45° alignment option dramatically reduces the need to adjust sensitivity gain by inherently matching the input magnitude observed for each axis. Some sensitivity mismatch may still be present, which might require minor adjustment.

This alignment was tested in the in-plane alignment at an identical range to the previous results. This alignment cannot use the CORDIC outputs from TMAG5170, given that it requires adjustment to the arctangent calculations to produce a useful result.

The resulting pre-calibrated error after performing phase correction is captured for this alignment and shown in 45° Angle Alignment Mechanical Angle Error

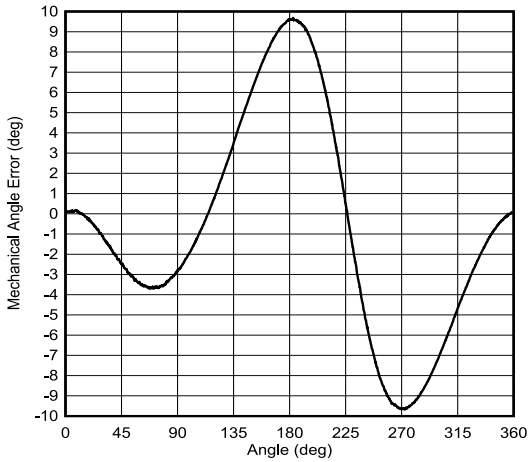

Figure 3-19. 45° Angle Alignment Mechanical Angle Error

Table 3-5. 45° Angle Alignment Harmonic Correction Factors

HARMONIC	α_i	β_i
1	–2.64	4.34
2	0.18	–5.59
3	0.82	0.51
4	–0.43	–0.05
5	0.06	–0.1
6	0	0.05
7	–0.025	–0.005

45° Calibrated Angle Error shows the resulting error after applying the harmonic data.

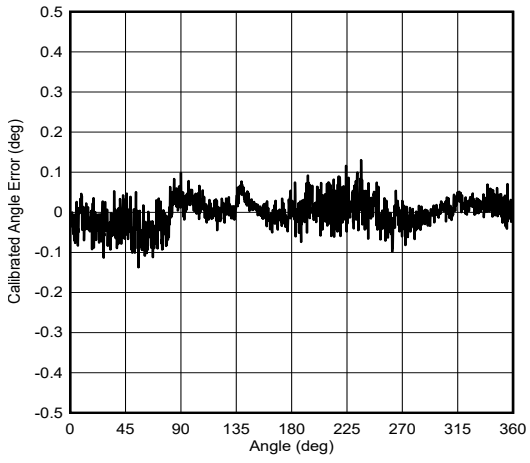

Figure 3-20. 45° Calibrated Angle Error

Copyright © 2022 Texas Instruments Incorporated

3.3.6 DRV5055 Off Axis Result

For this device, the sensitivity matching of the sensors requires some normalization by the controller before performing calculations on the captured analog data. This alignment requires sensors spread about the magnet by 90° and occupies more space than a single TMAG5170, and presents additional opportunity for mechanical misalignment. Despite these drawbacks, it is still possible to follow the same method of harmonic adjustment to eliminate angle error.

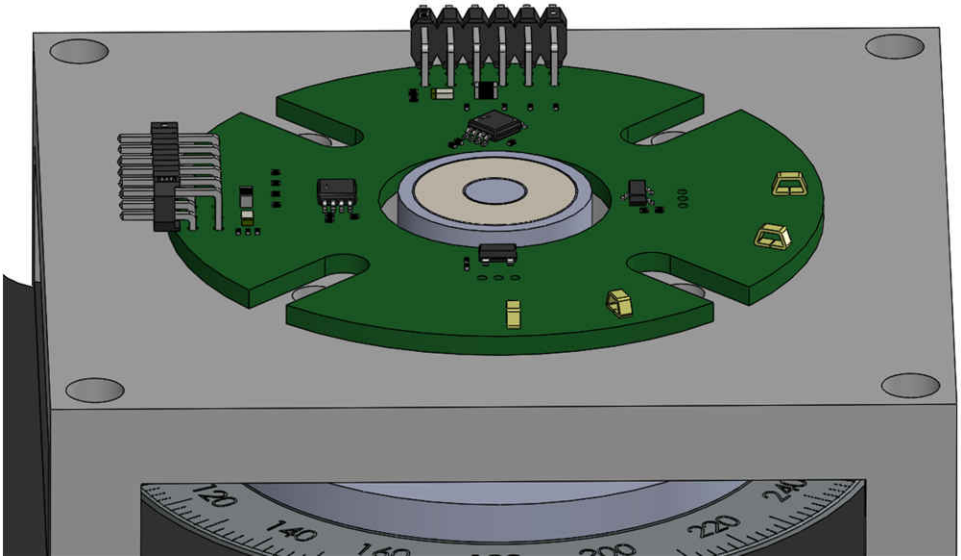

Figure 3-21. DRV5055 Off-Axis Configuration

DRV5055 Off-Axis Mechanical Angle Error shows the resulting pre-calibrated error captured for this alignment. The challenge observed using this configuration is that the number of mechanical errors possible in the system are now doubled with a second sensor. This produces a more complex error profile. Despite this, the same procedure for calibration applies and yields excellent results.

Figure 3-22. DRV5055 Off-Axis Mechanical Angle Error

Copyright © 2022 Texas Instruments Incorporated

HARMONIC	α_i	β_i
1	–7.3	0.35
2	1.17	0.22
3	–2.23	0.28
4	–0.81	–0.14
5	–0.075	0.01
6	–0.035	0.02
7	–0.03	–0.005
8	–0.01	0

DRV5055 Off-Axis Calibrated Angle Error shows the resulting error after applying the harmonic data.

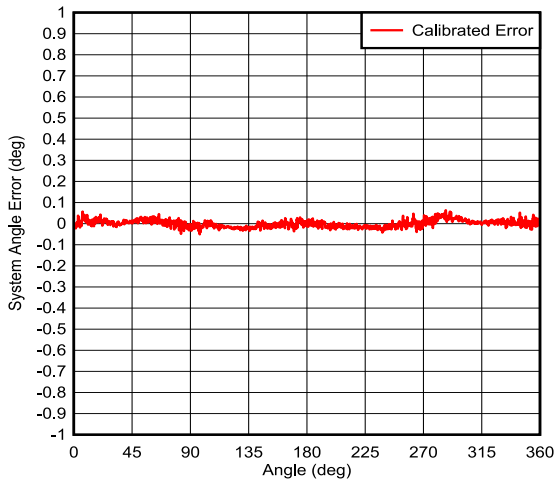

Figure 3-23. DRV5055 Off-Axis Calibrated Angle Error

Copyright © 2022 Texas Instruments Incorporated

4 Design and Documentation Support

4.1 Design Files

4.1.1 Schematics

To download the schematics and layout, see the design files at TIDA-060040.

4.1.2 BOM

To download the bill of materials (BOM), see the design files at TIDA-060040.

4.2 Tools and Software

Tools

TMAG5170UEVM GUI	The TMAG5170UEVM GUI offers a simple platform to configure device registers and monitor and record outputs of both TMAG5170A1 and TMAG5170A2.

4.3 Documentation Support

1. Texas Instruments, *TMAG5170 High-Precision 3D Linear Hall-Effect Sensor With SPI* data sheet
2. Texas Instruments, *DRV5055 Ratiometric Linear Hall Effect Sensor* data sheet

4.4 Support Resources

TI E2E™ support forums are an engineer's go-to source for fast, verified answers and design help — straight from the experts. Search existing answers or ask your own question to get the quick design help you need.

Linked content is provided "AS IS" by the respective contributors. They do not constitute TI specifications and do not necessarily reflect TI's views; see TI's Terms of Use.

4.5 Trademarks

TI E2E™ are trademarks of Texas Instruments.
All trademarks are the property of their respective owners.

Copyright © 2022 Texas Instruments Incorporated

IMPORTANT NOTICE AND DISCLAIMER

TI PROVIDES TECHNICAL AND RELIABILITY DATA (INCLUDING DATA SHEETS), DESIGN RESOURCES (INCLUDING REFERENCE DESIGNS), APPLICATION OR OTHER DESIGN ADVICE, WEB TOOLS, SAFETY INFORMATION, AND OTHER RESOURCES “AS IS” AND WITH ALL FAULTS, AND DISCLAIMS ALL WARRANTIES, EXPRESS AND IMPLIED, INCLUDING WITHOUT LIMITATION ANY IMPLIED WARRANTIES OF MERCHANTABILITY, FITNESS FOR A PARTICULAR PURPOSE OR NON-INFRINGEMENT OF THIRD PARTY INTELLECTUAL PROPERTY RIGHTS.

These resources are intended for skilled developers designing with TI products. You are solely responsible for (1) selecting the appropriate TI products for your application, (2) designing, validating and testing your application, and (3) ensuring your application meets applicable standards, and any other safety, security, regulatory or other requirements.

These resources are subject to change without notice. TI grants you permission to use these resources only for development of an application that uses the TI products described in the resource. Other reproduction and display of these resources is prohibited. No license is granted to any other TI intellectual property right or to any third party intellectual property right. TI disclaims responsibility for, and you will fully indemnify TI and its representatives against, any claims, damages, costs, losses, and liabilities arising out of your use of these resources.

TI’s products are provided subject to TI’s Terms of Sale or other applicable terms available either on ti.com or provided in conjunction with such TI products. TI’s provision of these resources does not expand or otherwise alter TI’s applicable warranties or warranty disclaimers for TI products.

TI objects to and rejects any additional or different terms you may have proposed.

Mailing Address: Texas Instruments, Post Office Box 655303, Dallas, Texas 75265
Copyright © 2022, Texas Instruments Incorporated